INSTITUTO SUPERIOR TÉCNICO
Universidade Técnica de Lisboa

# Analysis of bone remodeling in the tibia after total knee prosthesis

**Robalo, T.**
E-mail: tiago.robalo@ist.utl.pt

October 2011

**Abstract:** Total knee arthroplasty is a surgical treatment with one of the highest usage rate, making it the gold standard treatment for advanced osteoarthritis of the knee. However, knee prosthesis currently used still lack appropriate design solutions. The loss of bone in the tibia due to tibial component is one of the concerns about the success of the knee prosthesis. The purpose of the present work is to evaluate the bone remodeling that occurs in the tibia after total knee arthroplasty.

A three-dimensional model of the tibia was developed from CT images. The geometric modeling of the tibial components, as well as their discretization in finite elements (FE) were also made. Bone was modeled as a porous material characterized by its relative density at each point of the domain. The bone remodeling law was derived from a topology optimization problem, in which bone self-adapts in order to achieve the stiffest structure, being the total bone mass regulated by the metabolic cost associated with bone maintenance. By using the FE method together with the bone remodeling model developed in IST it was possible to analyze the physiological situation of bone, and also its behavior in different surgical scenarios.

The results showed that the distribution of bone densities around prosthesis' tibial component depends on the stem configuration and fixation mode. The use of long stems (cemented and uncemented) causes a clear stress shielding of the proximal tibia, leading to a significant reduction of bone density. It was also verified a high stress concentration close to the distal tip of the stem, with consequent hypertrophy of bone at the tip region. For short stems (standard) a tendency for maintaining bone remodeling process of the host bone close to physiological was noticed.

**Key-words:** Biomechanics; Total knee arthroplasty; Bone remodeling; FE method.

## 1. Introduction

The knee is one of the most often injured joints, since it is the most heavily loaded and one of the most mobile joints in the human body and is regularly subjected to great mechanical demands [1, 2]. For advanced arthritis, the treatment of choice is, generally, the knee replacement surgery, where the joint surface is replaced by an artificial implant [3], allowing the return to activities of daily living.

The total knee prosthesis is composed of femoral, tibial and patellar component. Tibial component can include a stem that inserts into the tibia, in order to obtain additional stability and fixation of the components, while allowing reconstruction of the bone defect [4]. This stem is available in a wide range of dimensions, designs and can be implanted in press-fit or cemented fashion. This variety of options maximizes the customizing of the implant to the patient and is essential to the success of the arthroplasty, protecting the limited bone stock remaining [5, 6, 7]. Shorter stems are used in primary total knee arthroplasty (TKA) surgery, while revision surgery may require longer stems [8].

Lately, several studies have described a significant decrease in postoperative bone mineral density (BMD) of tibia, adjacent to the implant, after TKA [9]. The prosthesis related bone loss is a concern about the success of the knee prosthesis, as it can lead to bone fracture and reduces the amount of bone available for the future revision surgery. This bone loss occurs mainly as a result of the phenomena of stress shielding (abnormal load distribution on the host bone), wear and implant loosening [6]. These events cause at long-term, a mechanical failure of the arthroplasty, with detachment of implants from bone support, thereby requiring the implantation of a new prosthesis [10].

The effect of stress shielding (shielding of bone from physiologic stress by implant components) is particularly important in the case of long stems, causing a reduction in bone density and strength that leads to TKA failure [11, 12]. The need of reoperation after revision TKA is approximately 15%, of which nearly 44% may require two or more additional surgeries [13]. Thus, understanding the bone adaptation process (alterations in bone mineral density and structure) with respect to the mechanical behaviour is a very important issue, especially in the choice of the right orthopaedic implant, allowing to improve implant performance and long-term outcomes [14]. An improvement in the design of the stem and in the means of fixing the stem to bone could minimize this phenomenon.

The finite element (FE) method has been widely used in orthopedic biomechanics to evaluate the mechanical behavior of biological tissues, particularly bone [15]. This method allows one to determine the stress or strain state of the bone tissue and to link that with biological processes like bone remodeling, through the combination of a mathematical model that simulates this behavior. This way it can be a useful tool to study the changes in bone adaptation due to the insertion of the tibial component prosthesis in the bone. Moreover, it is possible to estimate the amount of bone resorption related to a specific prosthesis design. Therefore, a better understanding of the biological and mechanical changes induced in bone tissue by prosthesis will allow surgeons to adopt the most appropriate solution for each patient.

The purpose of the present study is to better understand the biomechanical influence of the TKA in the process of bone remodeling that occurs in the tibia. It is intended to analyze the influence of the stem configuration (size of the stem) and mode of fixation (cemented/ cementless) in the existing bone loss due to the presence of tibial component implant. To do so the bone remodeling model developed in IST together with the FE method are applied in the implanted tibia model with three different tibial stem configurations (standard, cemented and press-fit), thus allowing to evaluate the process of bone adaptation. Stress analysis is also presented and, together with bone remodeling results are compared with experimental and clinical results obtained by other authors.

## 2. Model of bone remodeling

### *2.1 Optimization model*

Considering that bone adapts to the applied mechanical loading stiffening its structure, a model for bone remodeling can be derived from a topology optimization problem. A typical topology optimization model for elasticity problems consists in the process of distributing material by different regions, identifying solid or void regions (filled or without material, respectively), in order to obtain the stiffest structure within a given domain, i.e., the structure is identified by an optimal distribution of a material with variable relative density.

### *2.2 Material model for bone*

In this model, bone is modeled as a porous material with periodic microstructure, which is obtained by the repetition of unit cubic cells with prismatic holes, with dimension $a_1, a_2, a_3$, as shown in Figure 1. The bone relative density, $\mu$, at each point depends on local hole dimensions, i.e., $\mu = 1 - a_1 a_2 a_3$, with $a_i \in [0,1]$.

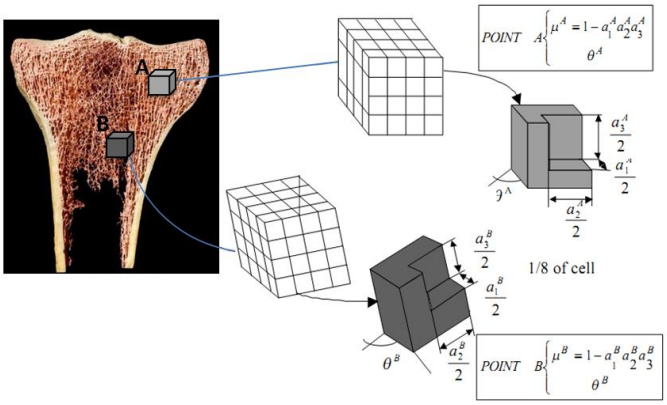


Figure 1 – Material model for bone, adapted from [16].

The extreme values $a_i = 0$, and $a_i = 1$ correspond to full material/compact bone and void/ without bone, respectively. For intermediate values, it corresponds to trabecular bone with variable porosity [14, 16, 17, 18].

The elastic properties of this material are calculated using homogenization methods.

### *2.3 Mathematical formulation*

The bone remodeling model consists in the computation of bone relative density (design variable), at each point of the domain, by solving an optimization problem, formulated in the continuum mechanics context. The optimization goal is to minimize, with respect to relative density, a linear combination of structural compliance (inverse of structural stiffness) and the metabolic cost to the organism of maintaining bone tissue [16, 17]. The solution for this problem yields the optimal distribution of bone density, i.e., the stiffest bone structure for the applied loads, as the bone adapts to the mechanical environment, with the total bone mass regulated by a parameter that quantifies the biological factors. Thus, the optimization problem reflects both mechanical advantage and metabolic cost [16, 17].

The bone remodeling problem considers bone (or implanted bone) as a structure occupying a volume $\Omega$, with fixed boundary $\Gamma_u$ and subjected to a set of surface

loads, f in the boundary $\Gamma_f$. The bone/stem and bone/cement interface are denoted by $\Gamma_c$ (see Figure 2) [17].

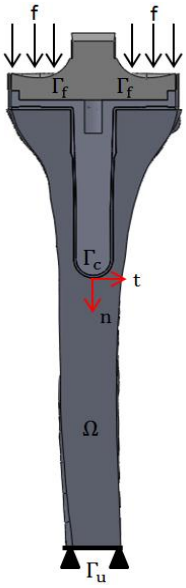


Figure 2 – Generalized elastic problem with contact, adapted from [17].

Defining the design variables $\boldsymbol{a} = \{a_1, a_2, a_3\}^T$, for each point as mentioned above and using a multiple load optimization criterion, the problem can be stated as:

$$\min_a \left\{ \sum_{P=1}^{NC} \alpha^P \left( \int_{\Gamma_f} {f_i}^P {u_i}^P d\Gamma \right) + k \int_\Omega \mu(\boldsymbol{a}) d\Omega \right\} \quad (1)$$

subjected to

$$0 \le a_i \le 1, \quad i = 1,2,3$$

$$\int_\Omega E^H_{ijkl}(\boldsymbol{a}) e_{ij}(\boldsymbol{u}^P) e_{kl}(\boldsymbol{v}^P) d\Omega - \int_{\Gamma_f} {f_i}^P {v_i}^P d\Gamma + \int_{\Gamma_c} {\tau_n}^P (v_n^{rel})^P + {\tau_t}^P (v_t^{rel})^P d\Gamma = 0 \quad (2)$$

$$\forall\, \boldsymbol{v}^p = 0 \; and \; \boldsymbol{u}^p = 0 \; on \; \Gamma_u$$

$$\begin{cases} (u_n^{rel})^P - g \le 0, \; {\tau_n}^P \ge 0, \; {\tau_n}^P ((u_n^{rel})^P - g) = 0 \;\; on \; \Gamma_c \\ |{\tau_t}^P| \le \vartheta |{\tau_n}^P| \rightarrow \begin{cases} |{\tau_t}^P| < \vartheta |{\tau_n}^P| \Rightarrow u_t^{rel} = 0 \\ |{\tau_t}^P| = \vartheta |{\tau_n}^P| \Rightarrow \exists \Lambda \ge 0 : u_t^{rel} = -\Lambda {\tau_t}^P \end{cases} \\ with \; P = 1, \dots, NC \end{cases} \quad (3)$$

where $NC$ is the number of considered load cases with the, respectively, load weight factors $\alpha^P$ satisfying $\sum_{P=1}^{NC} \alpha^P = 1$. The multiple load formulation allows considering different load cases corresponding to various types of daily life activities that body structures are often exposed to [17].

In the previous problem statement, Eqs. (2) and (3) corresponds to the set of equilibrium equations for two bodies in contact, in the form of a virtual displacement principle. In these equations, $E^H_{ijkl}$ is the homogenized material properties of bone, $e_{ij}$ is the strain field and ${v_i}^P$ the set of virtual displacements. The last term of Eq. (2) is the contribution of contact loads $\tau^P$, where the subscripts $n$ and $t$ denotes normal and tangential directions, respectively. In Eq. (3) $g$ is the gap between the two bodies and $\vartheta$ is the friction coefficient [17].

The objective function in Eq. (1) is based on the balance of two terms: the first term concerns to the weighted average of the work of applied forces, whereas the second term represents the metabolic cost of maintaining bone. The cost parameter, $k$, plays an important role, since the resulting optimal bone mass, not only depends on load values, but also depends strongly on cost parameter values, as demonstrated in [14].

For the resolution of the optimization problem formulated by equations (1-3) is used a Lagrangian method. The stationarity condition of the Lagrangian method with respect to the design variable $\boldsymbol{a}$ is

$$\sum_{P=1}^{NC} \alpha^P \frac{\partial E^H_{ijkl}}{\partial \boldsymbol{a}} e_{kl}(\boldsymbol{u}^P) e_{ij}(\boldsymbol{v}^P) + k \frac{\partial \mu}{\partial \boldsymbol{a}} = 0 \quad (4)$$

where $\boldsymbol{u}^P$ is the displacement field at equilibrium [16].

The law of bone remodeling is expressed by Eq. (4) and consists of the necessary condition for optimum that is solved by a suitable numerical procedure, through FE discretization, giving as result the distribution of bone density.

### *2.4 Computational model*

Computationally, the model is described by the following steps: initially, the homogenized elastic properties are computed for an initial solution ($\boldsymbol{a}_0$). Then, the set of displacement field, $\boldsymbol{u}^P$, are calculated by FE method using software ABAQUS®, according to the mechanical solicitation, solution of equilibrium equations (2) and (3). Based on the displacement field FE approximation, the necessary optimality condition (Eq. (4)), is checked. If satisfied (equal to zero) the process stops. If not, improved values of the design variables $\boldsymbol{a}$ are computed and the process restarts. The flowchart of the iterative process is shown in Figure 3.

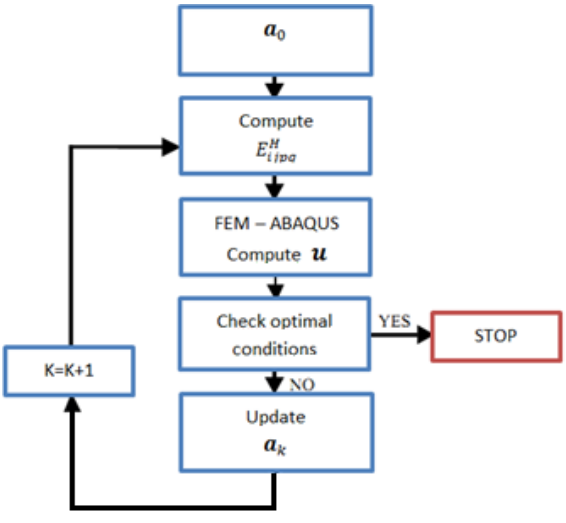


Figure 3 – Flowchart for the computational model procedure, adapted from [17].

In summary, this model is based on optimization strategies to computationally simulate the bone adaptation process modulated by mechanical forces, which was motivated by the original ideas of Wolff and others. In practical terms, this model takes into account the relationship between mechanical loads and metabolic activities that is directly related to bone architecture and, consequently, to the process of bone remodeling.

## 3. Adopted methodology – computational modeling

### *3.1 Geometric modeling*

#### *3.1.1 Intact tibia*

The 3-D anatomical model of the left tibia was obtained from Computed Tomography (CT) images using a geometric modeling pipeline (see Figure 4). The pipeline steps are: the medical images acquisition and segmentation; the surface mesh adjustments and, finally, the solid model generation. The resulting geometric model is suitable to generate the FE mesh, required for the study of bone remodeling and stress analysis.

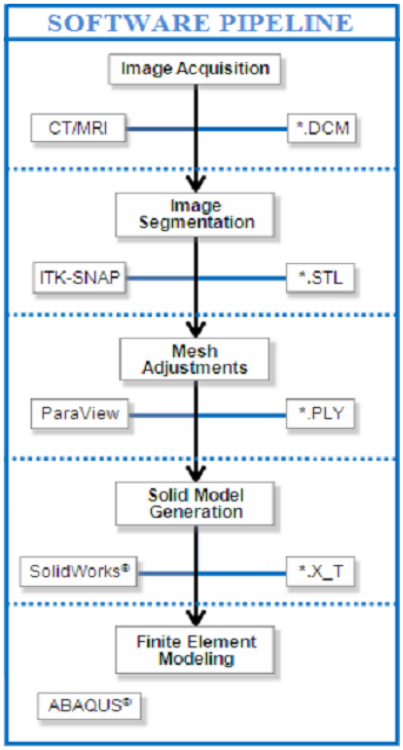


Figure 4 – Diagram of the geometric modeling pipeline, used to model the left tibia [19].

The input for the model's construction was CT images of a 43-year-old male subject without any local degeneration that were acquired from Osirix database.

The next modeling step is image segmentation, where three techniques were used in conjunction: global thresholding, active contour method and manual segmentation [19]. Firstly, thresholding technique is applied based on the images intensity values similarity. This allows distinguishing bone tissue from the background surrounding. The active contour method is a semi-automatic approach based on deformable surfaces, which adjust to the object boundaries during an iterative process. This is done taking into account the voxel probability maps derive from the thresholding technique. The obtained result by the active contour method is not totally accurate due to segmentation errors. Therefore it is necessary to use a manual segmentation technique. At the end, the segmentation output is a surface mesh of the anatomical structure.

After segmentation stage, the surface model is processed in order to improve the quality and computational efficiency of the geometric model. To do these, two different techniques were applied: smoothing (adjustment of the coordinates of mesh nodes) and decimation (simplification of surface mesh). The resulted surface mesh is presented in Figure 5.

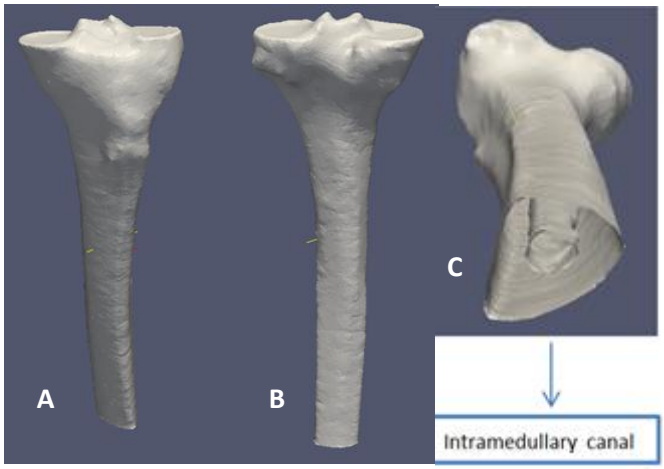


Figure 5 – Surface mesh model of the left tibia, result of the surface mesh adjustments stage: A – Anterior view; B – Posterior view; C – Inferior view.

This model is suitable to generate solid models of the anatomical geometry of the proximal tibia. For that, was used the commercial software SolidWorks® that includes the ScanTo3D® toolbox which automatically creates the solid model.

The obtained solid model was then imported to the software ABAQUS® to generate the FE mesh of it, so that it can be possible to do a computational analysis of the geometrical model.

#### *3.1.2 Bone with tibial prosthesis components*

After the modeling of the proximal left tibia, the solid models of the tibial components of TKA prostheses were developed. This modeling work was done using SolidWorks® software, based on real models and with the support of the P.F.C.® Sigma Knee System:

Technical Monograph [5]. The assembly results are presented in Figure 6.

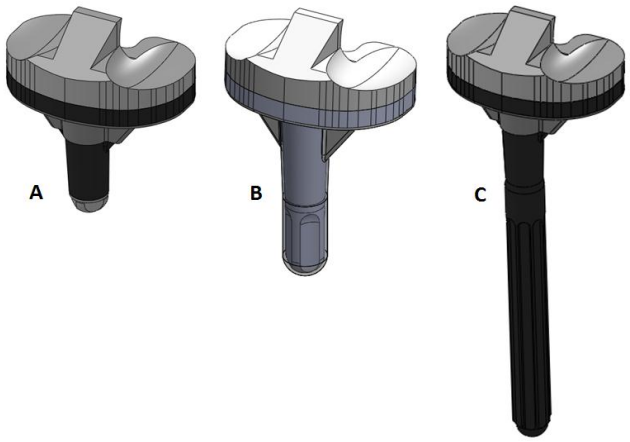


Figure 6 – Tibial components of TKA prostheses (stabilized insert, tibial tray, stem and cement mantle in superior third of the tibial tray for A and C, and involving the entire tibial tray and stem in B, with about 1 mm thickness): A – standard configuration; B – cemented configuration (30 mm length); C – press-fit configuration (115 mm length).

The last stage was to incorporate the assembled tibial components, for standard, cemented and press-fit configurations, into the bone with the accurate component alignment concern. The assembly results of all 3D models are shown in Figure 7.

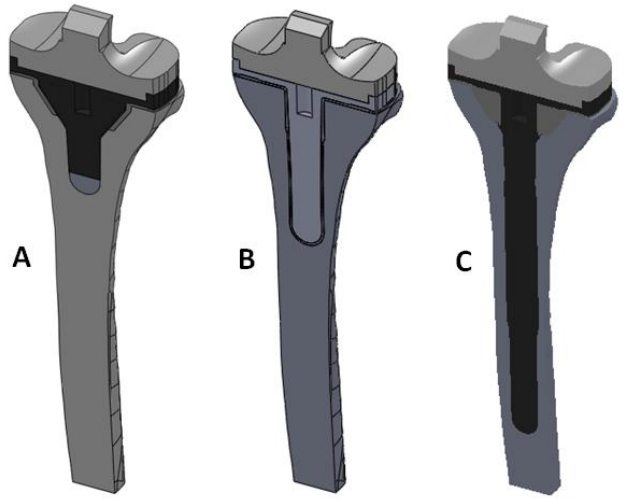


Figure 7 – Final assembly of the three different TKA constructs in the tibia: A – standard configuration; B – cemented configuration; C – press-fit configuration.

*3.2 Finite element method – FEM*

To perform the simulation of bone adaptation in a computational model, it is necessary to have a mathematical description of the process (as seen in section 2) combined with the finite element method (FEM). The FEM is a powerful technique developed to numerically solve a mathematical equation describing a physic phenomenon.

The FE analysis was performed by the commercial program ABAQUS®, which allowed for the: assignment of mechanical properties to the materials, contact formulation, application of loads and boundary conditions, and mesh generation.

*A. Material properties*

Table 1 contains the material properties assigned, which were assumed to be homogeneous, isotropic and with linear elastic behaviour, except for bone. Bone is modeled as a cellular material with an orthotropic microstructure, in which the relative density can vary along the domain and, is given by the material optimization process. The equivalent elastic properties for this material are computed using the homogenization method, as seen previously.

Table 1 – Material stiffness properties used in FE simulations [20].

| Component | Material | Elastic Modulus /GPa | Poisson's coefficient |
|---|---|---|---|
| **Compact bone** | | 17 | 0,3 |
| **Tibial tray and stems** | Titanium alloy | 110 | 0,3 |
| **Tibial insert** | UHMWPE | 0,5 | 0,3 |
| **Cement** | PMMA | 2,28 | 0,3 |

*B. Contact formulation, Boundary conditions and applied loads*

The contact between bone-cement, implant-cement and tibial tray-tibial insert was considered rigidly bonded for all the three TKA configurations [9, 21, 22, 23]. For the remaining contact between implant-bone, a coefficient of friction of 0,3 was used [24].

The lower extremity of the tibia was fixed with the boundary condition, called "encastre", and six different load cases were applied, using the multiple load criteria with equal weights (1/6), four correspond to the movement of level walking and, the remaining two concern to the deep knee bend movement. These six load cases were measured by an instrumented prosthesis and were based on the in vivo knee joint loading study developed by Bergmann, et al. 2010 [25, 26, 27].

Table 2 presents the six load cases considered representative of the range of loads that exist in these movements – acquired from Orthoload (K1L subject) [27]. These loads were applied in the FE analyses of this work, both in the natural knee as in all the three prostheses configurations. They were applied, on the upper surface of the cortical bone of the intact tibia (tibial plateau) and uniformly distributed, to the surface of each condyle of the tibial insert.

Table 2 – Forces and moments from level walking and knee bend applied in FE models [27].

| | Force/ N | | | Moment/ N.mm | | |
|---|---|---|---|---|---|---|
| | F1 | F2 | F3 | M1 | M2 | M3 |
| **Level Walking** | -76,05 | -318,9 | -169,96 | 2420 | -1900 | 3430 |
| | -144,65 | -1442,14 | 52,79 | 3760 | 1090 | -4790 |
| | -71,96 | -2141,34 | 61,18 | 8850 | 1070 | 20220 |
| | -20,16 | -2476,89 | 24,11 | 4760 | -10820 | 16990 |
| **Knee bend** | 75,8 | -2537,57 | -8,3 | 13220 | -2230 | 12030 |
| | -26,55 | -2801,01 | -292,26 | 17400 | -2790 | -7230 |

Forces directions relative to the tibial component: $F_1$, $F_2$ and $F_3$ act in medio-lateral, vertical and posterior-anterior, respectively. Moments $M_1$, $M_2$ and $M_3$ act in the sagittal, horizontal and frontal plane of the tibial component.

It must be further mentioned that these knee contact loads, acting in the implant, are only a fraction of the total load acting in the knee joint. Additional forces and moments transmitted from the femur to the tibia are transferred not only to the prosthesis, but also to tendons, ligaments and other soft tissues. However, as all these structures can only bear tensile forces, the loads obtained by the telemeterized implant are a good approach of the majority of the mechanical demands of the tibia, and do not constitute a limitation to this study.

*C. FE mesh generation*

At this stage were generated FE meshes of the geometric solid models of intact bone and of the implanted bones with the three tibial components prostheses (standard, cemented and press-fit), obtained in section 3.1. Table 3 presents the number of elements and nodes for each selected meshed model.

Table 3 – Number of elements and nodes of the FE meshes models.

| Model | Type of FE | Nº FE elements/nodes of the bone | Nº FE elements/nodes of the total assembly |
|---|---|---|---|
| **Intact bone** | 8-node hexahedral | 31840 / 34706 | - / - |
| **Standard configuration** | 4-node tetrahedral | 138569 / 26811 | 201706 / 42032 |
| **Cemented configuration** | | 142241 / 27779 | 214068 / 45483 |
| **Press-fit configuration** | | 161923 / 31876 | 246902 / 52078 |

*3.3 Analysis of the intact bone – Bone remodeling model tests*

Before applying the bone remodeling model to the implanted tibia, it was necessary to determine in advance the cost parameter $k$, which highly influences the amount of bone mass. This biological parameter was determined from the qualitative analysis of bone remodeling model applied to the intact bone (without implant).

Starting with uniform density distribution ($\mu$ = 0,3) various values of $k$ were tested. The most adequate value was $k$=0,003 N/mm$^2$, since it was the one that reproduced the morphology most similar to the real bone. After that, a second distribution of initial densities of intact bone, more similar to the reality than the uniform case was used for the input of bone remodeling model ($\mu$ = 0,05 for intramedullary canal, $\mu$ = 1 for a layer of cortical bone coating the tibia and $\mu$ = 0,3 for remaining nodes). The result of bone remodeling model is shown in Figure 8.

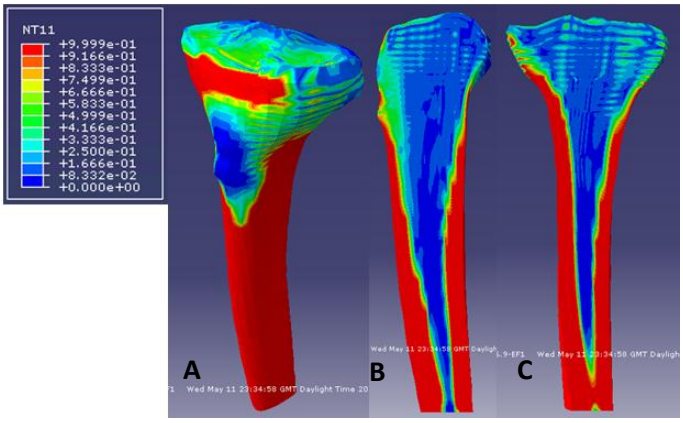


Figure 8 – Density distribution resulting from the model of bone remodeling for the initial non-homogeneous input with $k$=0,003 N/mm$^2$, step = 5 and 200 iterations. Relative densities, $\mu$, are represented in a color scale: red=cortical bone ($\mu \approx 1$) and the remaining=trabecular bone. A – Global view; B – Lateral section, right sagittal view; C – Frontal section, anterior view.

After the determination of the value of biomechanical parameter $k$, the evolution process of bone remodeling is applied to models with implant (standard, cemented and press-fit prosthesis), where only the bone is considered as design area and starting with the same density distribution as the obtained previously in the model of intact bone (Figure 8).

To evaluate the bone remodeling alterations, the implanted bone was divided into 6 different regions of same height (regions 1 to 6), which are in increasing order from the proximal extremity to the distal one, allowing to observe the remodeling process in more detail.

## 4. Results and discussion

The results of bone remodeling model for the different design solutions and mode of fixation (standard, cemented and press-fit), are presented in Figure 9, 10 and 11, respectively. In order to analyze the evolution of each of the density distributions, the starting point is also shown, which is similar in all cases.

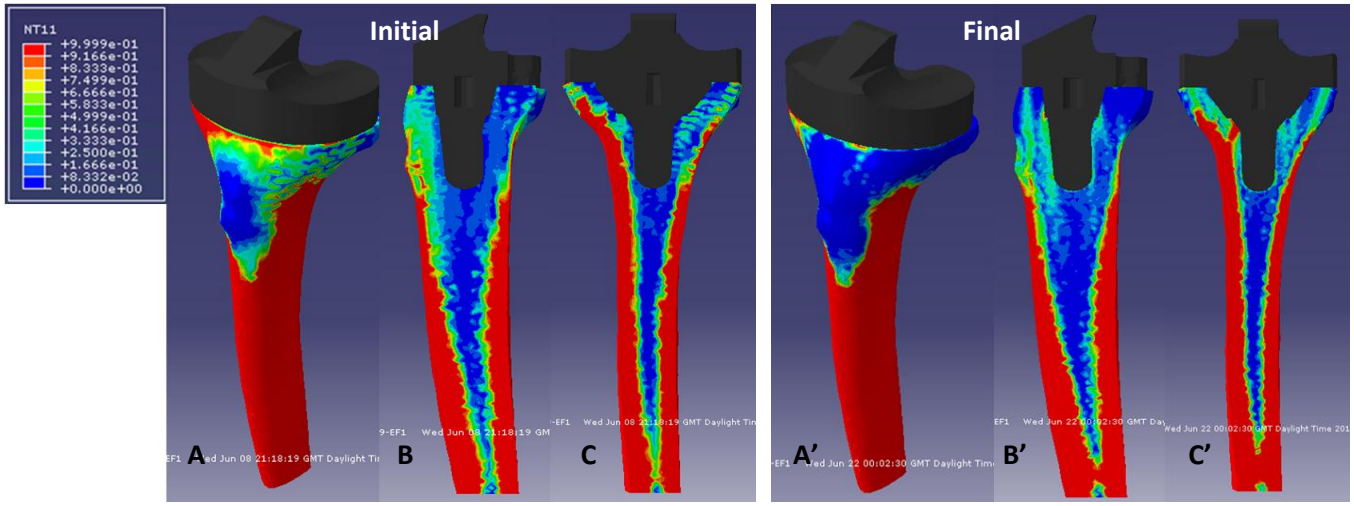


Figure 9 – Initial and final density distribution resulting from the model of bone remodeling for the implanted bone with standard prosthesis, at left and right, respectively. Relative densities, $\mu$, are represented in a color scale: red=cortical bone ($\mu \approx 1$) and the remaining=trabecular bone. A and A' – Global view; B and B' – Lateral section, right sagittal view; C and C' – Frontal section, anterior view.

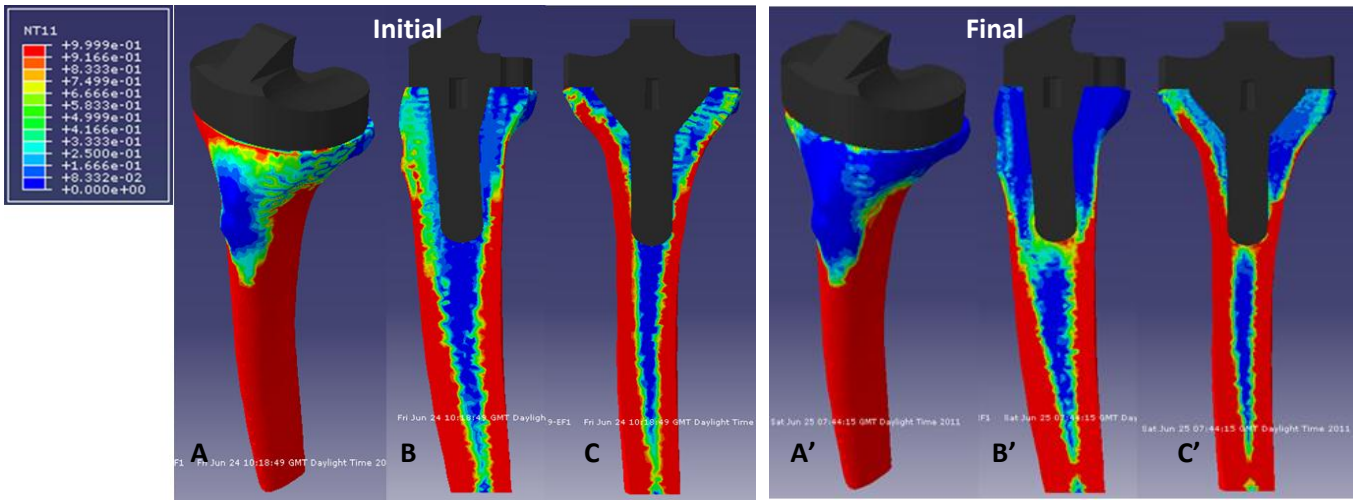


Figure 10 – Initial and final density distribution resulting from the model of bone remodeling for the implanted bone with cemented prosthesis, at left and right, respectively. Relative densities, $\mu$, are represented in a color scale: red=cortical bone ($\mu \approx 1$) and the remaining=trabecular bone. A and A' – Global view; B and B' – Lateral section, right sagittal view; C and C' – Frontal section, anterior view.

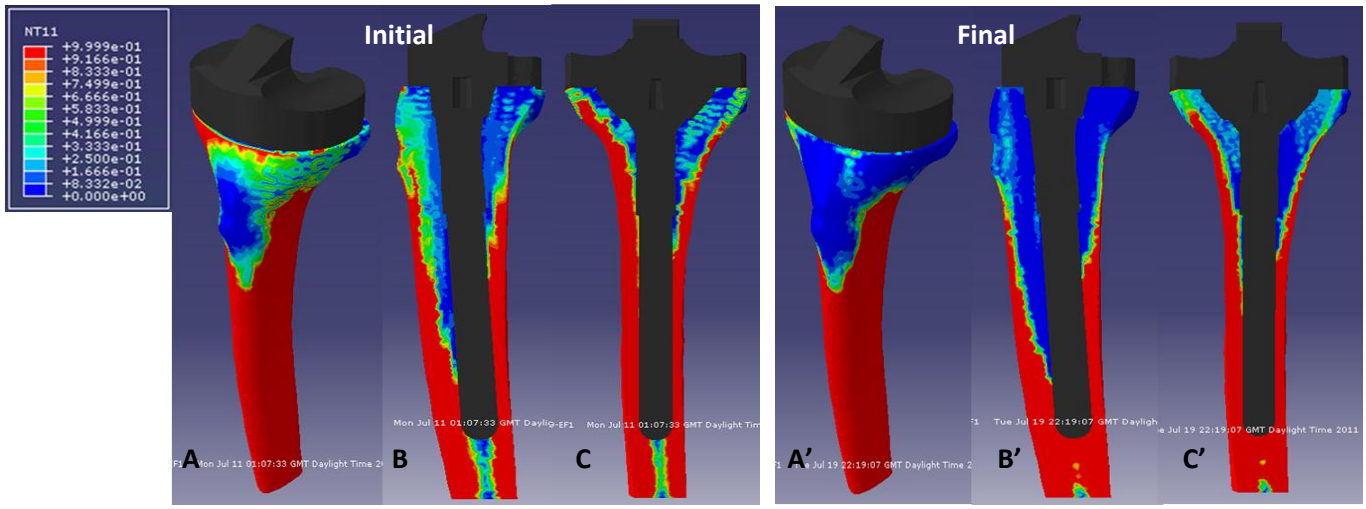


Figure 11 – Initial and final density distribution resulting from the model of bone remodeling for the implanted bone with press-fit prosthesis, at left and right, respectively. Relative densities, $\mu$, are represented in a color scale: red=cortical bone ($\mu \approx 1$) and the remaining=trabecular bone. A and A' – Global view; B and B' – Lateral section, right sagittal view; C and C' – Frontal section, anterior view.

Through the observation of the Figure 9 is possible to identify a small decrease of bone mass in the proximal region (region 1), especially in the thin surface layer of cortical bone that surrounds the bone and in the proximal posterior area. However, is also observed a modest densification of bone (increase in bone density) near the interface with prosthesis. For all the other regions (regions 2 to 6) no significant alterations of density distribution are shown.

By analyzing Figure 10 it is verified an elevated and generalized decrease of bone densities in the proximal regions adjacent to the prosthesis, namely regions 1 and 2. Nevertheless, in region 3 an increase of bone mass is shown in the area near the tip of the stem. For the remaining regions (4-6) there are no observable changes.

From Figure 11 it is possible to identify a severe and widespread loss of bone mass in the regions 1 to 4. However, in region 6 in the area which contacts with the tip of the stem it seems to exist a significant increase of densities of the nodes of the intramedullary canal. In region 5 there are no observable alterations.

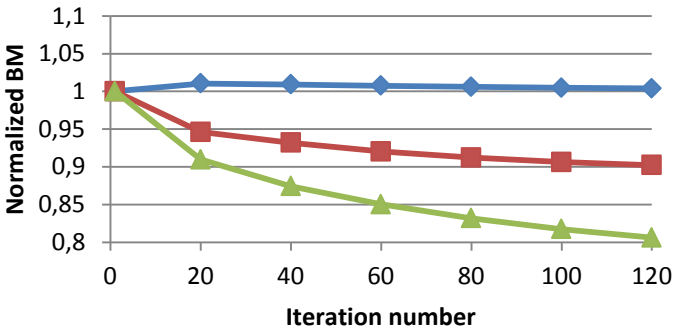


Figure 12 – Evolution of the total bone mass (BM) throughout the iterative process of bone remodeling, dimensionless by its initial mass: standard configuration (blue); cemented configuration (red); press-fit configuration (green).

In Figure 12 is shown the process of bone adaptation in global terms, i.e., the evolution of total bone mass (BM) throughout the iterative process. As it can be seen, for the standard configuration there is an almost negligible increase in total BM (0,4%). In the case of cemented configuration there is a decrease of -9,78% in total BM, due to the contribution of bone areas adjacent to the implant, more precisely in regions 1 and 2 (see Table 4). For the press-fit design there is a clear decrease in total BM (-19,39%), which suggests that exists a generalized weakening of the bone, a consequence of increased bone resorption over formation. This happens essentially because of a decrease in the densities of bone that are adjacent to the prosthesis. It should be noted that the process has reached the desired convergence within the number of iterations considered for all the three TKA constructs.

Table 4– Bone mass variation for the regions 1 to 6 and for the whole bone, result of the bone remodeling process, for the standard, cemented and press-fit prosthesis.

| | Bone mass variation (%) | | |
|---|---|---|---|
| | Standard | Cemented | Press-fit |
| Region 1 | -8,7379 | -41,6776 | -39,1660 |
| Region 2 | 3,0165 | -30,7143 | -42,2859 |
| Region 3 | 1,4059 | 4,8321 | -24,4517 |
| Region 4 | 1,6676 | 1,8224 | -9,0688 |
| Region 5 | 2,4695 | 2,8889 | 0,0537 |
| Region 6 | 2,8552 | 3,2284 | 3,7382 |
| Global | 0,4 | -9,78 | -19,39 |

Table 4 presents the percentage of BM variation for each of the regions in which the implanted bone was discretized. For the standard case is verified a not significant increase in BM in all the regions between 1 and 3%, except in the region 1, where the BM decreases (-8,74%). In the cemented case, is captured an accentuated loss of BM for the proximal region underneath the tibial tray until the proximal diaphysis (region 1 and 2), from about -40% to -30%. Furthermore, as seen previously there is a significant BM gain around the tip of the stem (region 3), about 5%. In all the other regions a slight and mostly not significant increase in BM is observed. For the press-fit design is verified an accentuated loss of BM for the regions 1 to 4. As we move away from the proximal region the bone loss decreases, with a BM variation from about -40% to -10%, until reach region 5 where no change in BM is noticed (around 0%). In region 6 there is even an increase in BM of about 4%. All these BM losses are translated into a decrease in total BM, as seen in Figure 12.

So, these results are consistent with those described above and allow inferring a possible existence of stress shielding effect in the bone for the cemented and press-fit configuration, since this effect is strongly correlated with the loss of bone density, i.e., this bone loss may reflect the bone response to altered mechanical loading conditions around the implant.

*A. Stress analysis*

To complement the bone remodeling analysis the Von Mises stresses were also evaluated for the FE models of intact and implanted proximal tibia for stemless (standard) and stemmed tibias (cemented and press-fit) – see Figure 13. These analyses are relative to the initial condition and to the third load case.

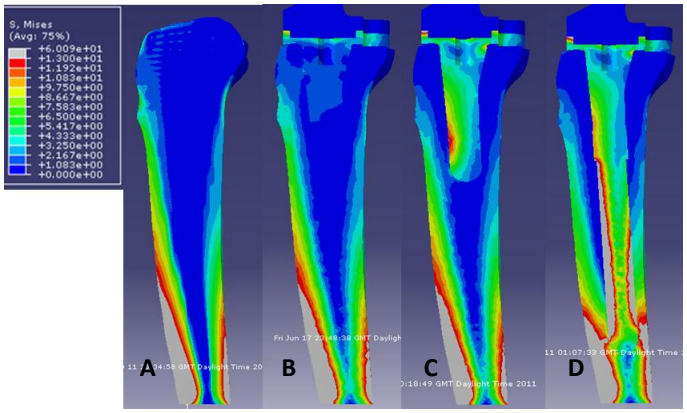


Figure 13 – Von Mises stresses for sagittal sections of bone and implant models: A – Intact tibia; B – Standard configuration; C – Cemented configuration; D – Press-fit configuration. Stresses represented in a color scale: grey=[13,60] MPa and the remaining=[0,13] MPa.

Comparing the stresses differences between the implanted and the intact tibia it is possible to notice a significant stress shielding effect (reduction of stresses relatively to intact tibia) in the proximal bone region close to tibial tray (region 1 and 2) in the stemmed tibias (Figure 13 C and D). The press-fit model presented this effect a bit more extensively along the stem and until about half of it.

This redistribution of stresses at the proximal level suggests a potential effect of bone resorption around the implant, due to osteclastic activity in a physiological environment for the cemented and press-fit configuration. It also helps to explain the result previously obtained with the bone remodeling model, in which was verified a decrease of bone mass in the proximal region adjacent to the prosthesis. These numerical findings corroborate the ones published by Lonner et al. [12] that used DEXA (dual energy X-ray) to determine bone density in the proximal region of tibias after TKA and confirmed that bone density was less at the regions under the tibial tray relative to the intact bone. They also are in agreement with the experimental studies of Completo et al. [6, 7] and with the work of Nyman et al. [28] who claim that the use of tibial components with long stems (120 mm press-fit stem) provoke greater bone loss until about half of the stem, which is in accordance with the levels of stress shielding found in this study.

This proximal bone resorption after TKA, due to phenomena of stress shielding, can cause a mechanical failure of the arthroplasty at long-term, with detachment of implants from bone support (tibial component loosening), which is a major and possibly increasing failure mechanism of TKA [11, 12], thereby requiring the implantation of a new prosthesis [10]. Thus, this bone loss may compromise the quality and outcome of a TKA revision.

In the present study the cemented configuration was the one who provoked less bone resorption in the metaphysis and proximal diaphysis of the bone, when compared to the press-fit stem which had the biggest loss of global BM, due to a bit more extensive stress-shielding effect along the stem. This may be explained by the difference in the stems length and not only on the fixation mode difference.

In contrast to the stemmed tibias, the standard stem configuration evidenced a tendency for maintaining the stresses experienced by the bone (see Figure 13 B), which can promote a physiological bone remodeling process of the host bone. This result is consistent with one previously obtained by the bone remodeling model, where no BM loss was recorded (except in region 1). These results also demonstrate a minor or absent effect of stress shielding with short stems relatively to the long stems for the cementless fixation mode, which is consistent with the study of Completo et al. [7]. So, one can conclude that apparently the length of stem is a major concern to proximally stress shielding effect. The increases on stem lengths, increase stiffness differences and, consequently, there are more significant changes in bone quality (loss of bone density).

In addition to the effect of stress shielding, also stress concentrations (increase of stress relatively to intact tibia) were assessed through FE analyses closely to the distal tip of stemmed tibias. These localized increase of stresses, can partially explain the clinical finding of pain, at the distal end of stem after revision TKA, especially for the long stem where the stress values increase more relative to the intact tibia. Haas et al. [29] described that 20% of patients with long stems had pain. Moreover, this augments of stress at stem tip can increase the risk of tibial fracture at this region and can induce hypertrophy of the cortical bone, i.e., the increase in loads on the bone stimulates osteoblastic activity locally and it is plausible an increase of locally bone density (ossification).

This same finding was captured in the density distribution resulting from the model of bone remodeling for the implanted bone with press-fit design (Figure 11) and, not so pronounced, with cemented prosthesis (Figure 10), where an increase of bone mass is shown in the area surrounding the stem tip. These results are once again in agreement with the results obtained at the University of Aveiro by Completo et al. [7] who studied the stress shielding through the FE analyses of different tibial stem designs.

Currently, there is a debate about the optimal design of the implant used in TKA procedure, in particular with respect to the configuration (stem length) and mode of fixation of the stem [30]. The reported alterations of proximal stress shielding and stress concentrations close to the distal tip, together with the consequent changes in bone adaptation, resulting from stemmed prosthetic implantation have become a clinical problem, compromising the stability of the implant and may contribute to prosthesis failure. The results of this study suggest that these problems are largely related with the use of stemmed tibial component (cemented and press-fit stem), in which a greater degree of bone loss is obtained compared to the un-stemmed design (standard), due to decreased proximal loading. This fact may explain the excellent long-term results generally achieved with standard configuration in primary TKA and makes this design the most advisable when carrying out TKA. However, this is only possible when the bone quality allows fixing the prosthesis, which is generally not the case when performing a revision TKA surgery, where the limited bone stock remaining requires the stemmed augments to improve fixation, alignment and stabilize the implant, enhancing the resistance to lift-off and shear [30].

In summary, knee prosthesis is a device that still lacks of adequate design solutions. These bone adaptation alterations due to the insertion of tibial component can play an important role on the longevity of present TKA designs and are a key factor in their failure. Thus, the previously reported knowledge of the mechanical behavior of the implant-bone set is very important to predict the performance of the prosthesis and can be a useful adjunct for the design of future implants, possibly, providing better conditions for longevity of the tibial component.

## References


[1] Tortora, G. and Derrickson, B., *Principles of anatomy and physiology*. 12th ed. 2009: John Wiley & Sons, Inc.

[2] Darrow, M., *The Knee Sourcebook*. 1st ed. 2002: McGraw-Hill.

[3] NIH Consensus Statement on total knee replacement. NIH Consens State Sci Statements 2003 Dec 8-10;20(1):1-34.

[4] Myman, J., Hazelwood, S., Rodrigo, J., *Long Stemmed Total Knee Arthroplasty With Interlocking Screws: A Computational Bone Adaptation Study.* University of California.

[5] *P.F.C Sigma Knee System: Technical Monograph*. 2000, England: DePuy International Ltd.

[6] Completo, A., Rego, A., F. Fonseca, J.A. Simões, *Strain shielding in proximal tibia of stemmed knee prosthesis: Experimental study.* Journal of Biomechanics (2007), doi:10.1016/j.jbiomech.2007.10.006.

[7] Completo, P.,Talaia, A., F. Fonseca, J.A. Simões, *Relationship of design features of stemmed tibial knee prosthesis with stress shielding and end-of-stem pain.* Materials and Design 30 (2009) 1391–1397.

[8] Gamelas J., Artroplastias totais do joelho. *Estudo comparativo de dois métodos de alinhamento no posicionamento do componente tibial*. Tese de Doutoramento, FCMUNL, Lisboa, 2006.

[9] Completo, A., Rego, A., F. Fonseca, A. Ramos, C. Relvas, J.A. Simões, *Biomechanical evaluation of proximal tibia behaviour with the use of femoral stems in revision TKA: An in vitro and finite element analysis*. Clinical Biomechanics 25 (2010) 159–165.

[10] Judas, F., Costa, P., Teixeira, L., *Procedimentos cirúrgicos do joelho na artrite reumatóide.* Acta Reum. Port. 2007;32:333-339.

[11] Anthony, G., Raso, V., Liggins, A., Amirfazli, A., *Contribution of loading conditions and material properties to stress shielding near the tibial component of total knee replacements.* Journal of Biomechanics 40 (2007) 1410–1416.

[12] Lonner JH, Klotz M, Levitz C, Lotke PA. *Changes in bone density after cemented total knee arthroplasty: influence of stem design.* J Arthroplasty 2001;16(1):107–11.

[13] Sierra, R.J., Pagnano, M.W., Trousdale, R.T., *Reoperations after 3200 revision total knee replacements: rate, etiology, and lessons learned*. In: Proceedings of the 70th Annual Meeting of the AAOS. New Orleans, (2003) p. 40.

[14] Fernandes, P., Rodrigues, H., Jacobs, C., *A model of bone adaptation using a global optimisation criterion based on the trajectorial theory of Wolff*. Comput Methods Biomech Biomed Engin. 1999;2(2):125-138.

[15] Completo, A., Rego, A., F. Fonseca, J.A. Simões, *Modelo numérico e experimental da tíbia intacta e com componente tibial da prótese do joelho.* Universidade de Aveiro.

[16] Fernandes, P., Rodrigues, H., *A material optimization model for bone remodeling around cementless hip stems.* ECCM'99 (1999).

[17] Femandes P. R., Folgado J., Jacobs C and Pellegrini V., *A contact model with ingrowth control for bone remodelling around cementless stems.* Journal of Biomechanics 35(2) (2002) pp. 167-176.

[18] Fernandes, P., Rodrigues, H., *Optimization models in the simulation of the bone adaptation process*, "Computational Bioengineering Current trends and applications", M. Cerrola, M. Dobalré, G. Martínez, B. Calvo, Imperial college press (2004).

[19] Ribeiro, N., Fernandes, PC, Lopes, DS, *3-D solid and finite element modeling of biomechanical structures – A software pipeline.*7th EUROMECH Solid Mech.Conference (2009).

[20] Completo, A., J.A. Simões, F. Fonseca, *The influence of different tibial stem designs in load sharing and stability at the cement-bone interface in revision TKA.* The Knee 2008.15:p.227-232.

[21] Mann, K., Bartel, D., Wright, T., *Coulomb frictional interfaces in modeling cemented total hip replacements: a more realistic model.* J. Biomechanics. Vol. 28.No.9.1067-1078.(1995).

[22] Jeffers, J., Browne, M., *Cement mantle fatigue failure in total hip replacement: Experimental and computational testing.* Journal of Biomechanics 40 (2007) 1525–1533.

[23] Huiskes, R., Verdonschot, N., *The effects of cement-stem debonding in THA on the long-term failure probability of cement.* J. Biomechanics Vol.30 No.8, pp. 795-802, 1997.

[24] Viceconti, M., Muccini, R., *Large-sliding contact elements accurately predict levels of bone implant micromotion relevant to osseointegration.*Journal of Biomechanics 33 (2000) 1611 1618

[25] Kutzner, I., Heinlein, B., F. Graichen, A. Bender, A. Rohlmann, A.M. Halder, A. Beier, and G. Bergmann, *Loading of the knee joint during activities of daily living measured in vivo in five subjects*. J Biomech. 2010 Aug 10;43(11):2164-73.

[26] Heinlein, B., I. Kutzner, F. Graichen, A. Bender, A. Rohlmann, A.M. Halder, A. Beier, and G. Bergmann, *ESB Clinical Biomechanics Award 2008: Complete data of total knee replacement loading for level walking and stair climbing measured in vivo with a follow-up of 6-10 months*. Clin Biomech (Bristol, Avon), 2009. 24(4): p. 315-326.

[28] Nyman JF, Hazelwood SJ, Rodrigo JJ, *Long stemmed total knee arthroplasty with interlocking screws: a computational bone adaptation study.* J Orthop Res 2004;22:51–8.

[29] Haas SB, Insall JN, Montgomery W, Windsor RE. *Revision total knee arthroplasty with use of modular components with stems inserted without cement.* J Bone Joint Surg Am 1995;77:1700–7.

[30] Whittaker, J., Dharmarajan, R., *The management of bone loss in revision total knee replacement.*J Bone Joint Surg [Br] 2008;90-B:981-7.